Sebacic acid/CNT sponge phase change material with excellent thermal conductivity and photo-thermal performance

Qi Zhang[a,b], Jian Liu[a,*]

[a] Key Laboratory of Distributed Energy Systems of Guangdong Province, Department of Energy and Chemical Engineering, Dongguan University of Technology, Dongguan 523808, China
[b] Key Laboratory of Ehanced Heat Transfer and Energy Conservation, the Ministry of Education, School of Chemistry and Chemical Engineering, South China University of Technology, Guangzhou 510640, China

ARTICLE INFO

ABSTRACT

Latent heat thermal energy storage system using phase change materials was widely used in solar thermal systems. Here, a novel form-stable phase change composite was successfully prepared. The sebacic acid is encapsulated by carbon nanotube sponge. The as-prepared composite is determined by SEM, FT-IR and XRD and the results show that the paraffin is mostly encapsulated in the pores of carbon nanotube sponge. The DSC measurements indicate that the melting temperature and latent heat of the composite are 121.1 °C and 131.8 J g^{-1}, respectively. The phase change composite could maintain its phase transition perfectly after 200 melting−freezing cycles, and no leakage of sebacic acid was observed by further SEM observation. The as-prepared composite shows 27-fold thermal conductivity enhancement as compared to the pure sebacic acid. Further, the as-prepared composite shows great photo-thermal performance when under simulated solar irradiation. Hence, the carbon nanotube sponge based high temperature phase change composite has great potential in solar thermal application.

1. Introduction

Efficient and reliable storage systems for solar thermal energy are an important requirement. Latent heat thermal energy storage (LHTES) system using phase change materials (PCMs) is a process near isothermal that can provide significantly larger storage capacity compared to sensible heat thermal energy storage (SHTES) at the same temperature range [1]. The LHTES incorporating PCM will comprise significantly smaller volume when compared to other materials storing only sensible heat [2]. A further advantage of latent heat storage is that heat storage and delivery normally occur over a fairly narrow temperature range the phase change temperature [3]. In solar thermal application, the PCMs generally refers to the materials (organic and inorganic) with melting temperature higher than 80 °C [4,5]. Higher melting temperature of PCMs has an advantage of obtaining higher efficiency of the LHTES.

In general, the PCMs can be broadly classified into two types: organic and inorganic. Inorganic PCMs include salt hydrates [6], salts [7], metals [8] and alloys [9], whereas organic PCMs are comprised of paraffin [10,11], fatty acids/esters [12,13] and polyalcohols. Among the investigated PCMs, organic PCMs is chemically inert and stable, shows little volume change and low vapor pressure in the melting form,

also it is nontoxic and non-corroding [14]. Hence, the organic PCMs are taken as the most promising phase change material. However, the direct utilization of these organic PCMs for heat storage is subject to some restrictions because of their leakage during the solid−liquid phase transitions. In order to prevent the leakage during the solid–liquid phase change of the paraffin, there have been intensive efforts in exploring potential encapsulation methods for organic PCMs [15]. The methods of encapsulation can be classified into two types: chemical and physical. Between the two methods, physical method is widely used since it is simple and do not disrupt the structure of PCMs. Up to now, a lot of porous and robust materials are used to physically encapsulate organic PCMs. For instance, the impregnation of paraffin in expanded graphite [16,17] or aerogel [18]. Among the porous materials, the carbon based materials could not only encapsulate the organic PCMs, but also improve the thermal conductivity of the PCMs.

In this paper, a new porous cabon based material carbon nanotube sponge (CNT sponge) was used to encapsulate a high temperature phase change material sebacic acid (SA). The SA was impregnated into the CNT sponge and easily absorbed by the pores of CNT sponge. The characterization of structure and properties of the prepared composites show that the phase change composite both have good formability, high heat storage capability, high thermal conductivity and photo-thermal
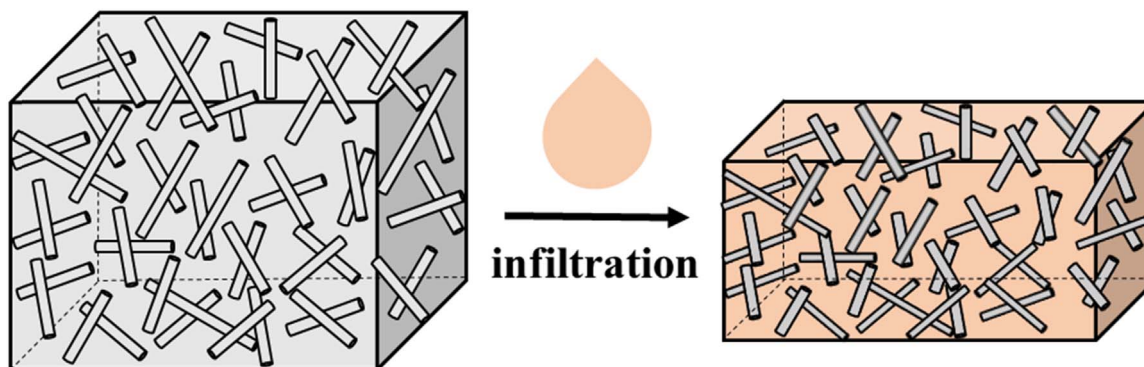
Fig. 1. The preparation of SA/CNT sponge.

performance, thus have great potential in practical application.

2. Experimental

2.1. Materials

Technical grade Sebacic acid (SA) was purchased from Beiyatekeji Chemical Co, Ltd. The CNT sponge was supplied by Nanjing XFNANO Materials Tech Co., Ltd.

2.2. Preparation of SA/CNT sponge composite

As shown in Fig. 1, the SA was placed in a thermostat with temperature of 150 °C and melted to liquid, then, the CNT sponge was immersed into the liquid SA to encapsulate the SA. After certain minutes, the composites were refloated followed by filtered and dried, the SA/CNT sponge phase change composite was obtained. To evaluate the absorbability of CNT sponge, different immersion time was conducted in the preparation process.

2.3. Characterizations of SA/CNT sponge composite

The morphology and microstructure of CNT sponge and SA/CNT sponge composite were observed on a field emission scanning electron microscopy (SU8020, Hitachi). The hexagon pores of the CNT sponge was observed by a transmission electron microscopy (FEI Tecnai G20). The surface area (S_{BET}), pore volume (V_{pore}) and pore size (D_{pore}) were tested by Brunauer–Emmett–Teller (BET) method. The structure of the composite was characterized by FT-IR spectra and X-ray diffraction. The FT-IR spectra were recorded on a Bruker 550 from 400 to 4000 cm^{-1} using KBr pellets, the X-ray diffraction (XRD) patterns of the samples were carried out on X-ray diffractometer (D8 ADVANCE). The phase change temperature and latent heat of the samples were measured by a differential scanning calorimeter (Q20, TA). For DSC measurements, 5–8 mg for every sample was sealed in an aluminum pan for characterization at a heating rate of 10 °C min^{-1} under a constant stream of nitrogen at flow rate of 50 mL min^{-1}. The thermal stability of CNT sponge and the SA/CNT sponge composite PCM was investigated by the thermogravimetric analysis (TGA) using a thermal analyzer (Q600 SDT, TA, URT100). The measurements were conducted by heating the samples from room temperature to 600 °C at a heating rate of 10 °C min^{-1} under nitrogen atmosphere with a flow rate of 100 mL min^{-1}. The thermal conductivities of the obtained round block was measured using a thermal constants analyzer (Hot Disk TPS 2500S, Hot Disk AB, Sweden). For comparison purpose, SA was melted and poured into the cylindrical mold to fabricate two pieces of casting samples so as to measure the thermal conductivity of SA.

The photo-thermal conversion performance of SA/CNT sponge composite was conducted under simulated solar irradiation. As shown in Fig. 2, the experimental apparatus consists of the photo-thermal

conversion system and the data collection system. In this experiment, the samples were loaded in aquartzose beaker under the solar simulator (Microsolar300, Perfectlight), the heat storage was carried out when the light was turned on. After the temperatures of the samples reached ~ 140 °C, the light was turned off and the samples were immediately cooled to room temperature, during which the samples under went a heat release process. The temperature of the samples during these periods were recorded by a thermal infrared imager (Ti 9, Fluke, ± 0.1 °C). An irradiatometer(ST-80C, Photoelectric Instrument Factory of Beijing Normal University) was used to measure and verify the power of the light irradiation from a simulated light source.

3. Results and discussion

3.1. Characterization of SA/CNT sponge composite

The morphology and microstructure of CNT sponge and the SA/CNT sponge composite are observed by SEM. As shown in Fig. 3a, b, the messy cabon nanotubes form porous CNT sponges via cross-linking and twining. The pore diameter of CNT sponge ranges from several hundreds of nanometer to several micrometer. The pores of the CNT sponge could absorb the SA to for form composite PCM. Fig. 3c,d show that the SA/CNT sponge composite. The mesopores of the CNT sponge were filled and the carbon nanotubes were expanded by impregnating the SA via capillary force and surface tension.

To further confirm the tube structure of SA/CNT sponge, the FT-IR and XRD spectrums of the phase change composite are conducted. The FT-IR spectra of SA, CNT sponge and the composite PCM are displayed in Fig. 4. In the spectrum of SA, the peaks at 2956 and 2917 cm^{-1} correspond to the stretching vibration of $-CH_3$, and 2850 cm^{-1} is ascribed to the stretching vibration of $-CH_2-$. The peak at 1697 cm^{-1} represents the stretching vibration of the C=O group. The peak at 1421 cm^{-1} is assigned to the bending vibration of the -CH$_2$ group. The peak at 720 cm^{-1} represents the swinging vibration of the CH$_2$ group, a feature of (CH$_2$)$_8$. The spectrum of the CNT sponge shows bands that are assigned to the vibrations of the carbon structure, namely the band at 1565 cm^{-1} assigned to C=C stretching vibrations of the aromatic carbon and the band centered at 1130 cm^{-1} which has contributions from the skeletal C=C tangential motions. The low intense bands at 3400 cm^{-1} is assigned to O-H stretching vibrations from phenol groups [19]. In the spectrum of SA/CNT sponge composite, the peaks assigned to CNT sponge at 3400, 1565 and 1130 cm^{-1}, and the peaks assigned to paraffin at 2956, 2917, 2850, 1697, 1421 and 720 cm^{-1} still existed, and no significant new peak is observed, which confirms that the tube structure of the SA/CNT sponge composite, also reveals the composite material are physical interaction.

The XRD patterns of the SA, CNT sponge and SA/CNT sponge composite are displayed in Fig. 5. In the pattern of SA, the strong diffraction peaks at 2θ = 8.1°, 21.5°, 24.1°, 26.5°, 30.1°, 43.2° and 51.6° were caused by regular crystallization of the pure SA. In the pattern of